Journal of Solid State Chemistry 183 (2010) 504–509

Contents lists available at ScienceDirect

Journal of Solid State Chemistry

journal homepage: www.elsevier.com/locate/jssc

Site preference and vibrational properties of $R_3T_{4+x}Al_{12-x}$ (R=Y, Ce, Gd, U, Th; T=Fe, Ru)

Yi Chen [a,*], Jiang Shen [a], Nan-xian Chen [a,b]

[a] Institute of Applied Physics, University of Science and Technology Beijing, Beijing 100083, China
[b] Department of Physics, Tsinghua University, Beijing 100084, China

ARTICLE INFO

Article history:
Received 17 October 2009
Received in revised form
16 December 2009
Accepted 20 December 2009
Available online 4 January 2010

Keywords:
Actinide compounds
Site preference
Lattice dynamics

ABSTRACT

The crystal structures and phase stability of the ternary alloys $R_3T_{4+x}Al_{12-x}$ (R=Y, Ce, Gd, U, Th; T=Fe, Ru) have been investigated using the interatomic potentials obtained by the lattice inversion method. These compounds crystallize in the hexagonal $Gd_3Ru_4Al_{12}$-type structure and the calculated lattice constants correspond well with the experiments. Among the four different kinds of Al sites in the structure, the most preferential sites for Fe atoms or Ru atoms are 6*h* sites. The properties related to lattice vibration, such as the phonon density of states (DOS) and Debye temperature of $R_3Fe_4Al_{12}$ have been evaluated. A qualitative analysis is carried out with the relevant potentials for the vibrational modes, which makes it possible to predict some thermodynamic properties.

1. Introduction

During the past few years, ternary alloys and intermetallic compounds of the *R*–*T*–Al systems (*R*=rare earth; *T*=transition metal) have received considerable attention from the materials community. These aluminides exhibit distinctive physical properties such as the coexistence of magnetism and superconductivity, heavy-fermion behavior, or valence fluctuations [1–3]. Since the discovery of $Gd_3Ru_4Al_{12}$ compound by Gladyshevskii et al. [4], a number of Ru-based and Os-based aluminides had been synthesized in 2002 [5]. More recently, several groups have focused their attention on the Fe-based and Co-based aluminides, and the *R* element extend from lanthanide to the actinide [6–10]. It has been found that $U_3Fe_{4+x}Al_{12-x}$ is a good candidate for a spin-glass-like behavior system due to the ordered geometrical configuration [9,10]. The $R_3T_4Al_{12}$ ternary compounds crystallize in a hexagonal structure (S.G. $P6_3/mmc$) with seven different crystallographic positions: *R* (lanthanide or actinide) atoms occupy the $6h_1$ sites, whereas *T* (transition metal) and Al atoms are located at the 2*a*, 6*g*, 2*b*, 4*f*, 6*h* and 12*k* symmetry sites. The *T* atoms can substitute for Al atoms up to a rather large extent in the ternary phases, and the site preferences are of particular interest during the substitution. According to Concalves's X-ray powder diffraction analysis of $U_3Fe_{4+x}Al_{12-x}$, the positions for Fe atoms substituting Al atoms are 12*k*, 6*h* and 4*f* sites, most likely 6*h* site [10]. One purpose of this work is to investigate the site preference from the viewpoint of energy. It is accepted that the local atomic environment determines whether the energy of a compound is low enough to form a stable structure with a certain type. To our knowledge, the thermodynamics properties of these ternary aluminides have not been reported up to now. In this work, the lattice constants, phases stability, phonon density of states, specific heat, vibrational entropy and Debye temperature of the $R_3T_{4+x}Al_{12-x}$ (R=Y, Ce, Gd, U, Th; T=Fe, Ru) compounds have been investigated by atomistic simulations with a series of effective potentials.

2. Methodology

Large-scale atomistic simulations have been widely used in investigating the properties and behaviors of different materials with complex structures. One of the key problems is how to obtain the effective potentials to describe the interaction between atoms. Some empirical or semi-empirical potentials, such as Lennard–Jones potential, embedded-atom-method potential, and tight-binding Gupta-type potential, etc., are often employed [11]. There are many adjusting parameters in the formalism of these potentials and the adjusting parameters are usually determined by fitting to some experimental data of the systems involved, for instance, the lattice constant, cohesive energy, elastic constants, vacancy formation energy and so on. Sometimes, it is hard to obtain some reliable experimental data such as the elastic modulus of the brittle materials and the single vacancy formation that may differ with the different experimental techniques employed [12]. Furthermore, the potentials between

* Corresponding author. Fax: +86 10 62322872.
E-mail address: chenyiustb@yahoo.cn (Y. Chen).

0022-4596/$ - see front matter © 2009 Elsevier Inc. All rights reserved.
doi:10.1016/j.jssc.2009.12.022

actinide atoms and transition metal atoms are few in the literature.

In this paper, the interatomic potentials are derived directly from the cohesive energy curves based on the lattice inversion method. The technique used for obtaining the *ab initio* pair potential was initially proposed by Carlsson, Gelatt and Ehrenrchich (CGE) [13]. However, the expression for their solution includes infinite summations, each of which includes infinite terms, making it inconvenient for analysis. Chen et al. used the Mobius-inversion formula in number theory to obtain pair potentials not only for the pure metals, but also for the intermetallic compounds with faster convergence than the CGE method [14–16]. A brief introduction to this method is given as follows.

2.1. Acquisition of cohesive energy curves

In order to obtain the necessary interatomic potentials, some simple and virtual structures are designed. Here we take a single crystal as an example to explain how to calculate the partially cohesive energies. The partial cohesive energy of distinct atoms $E_{Ru-Al}(x)$ could be obtained from a B2 or CsCl structure:

$$E_{Ru-Al}(x) = E^{B2}_{Ru-Al}(x) - E^{SC}_{Ru}(x) - E^{SC}_{Al}(x) \quad (1)$$

Here x is the nearest neighbor distance in the B2 structure, $E^{B2}_{Ru-Al}(x)$ represents the total energy curve with the B2 structure, and $E^{SC}_{Ru}(x)$ or $E^{SC}_{Al}(x)$ is the total energy function with the SC structure. In addition, the partial cohesive energy of identical atoms $E_{Al-Al}(x)$ could be obtained from a BCC structure if we consider a BCC Al structure as a B2 structure with two simple cubic (SC) sub-lattices Al_1 and Al_2:

$$E_{Al-Al}(x) = E^{BCC}_{Al}(x) - E^{SC}_{Al_1}(x) - E^{SC}_{Al_2}(x) \quad (2)$$

Here $E^{BCC}_{Al-Al}(x)$ represents the total energy curve with the BCC structure, and $E^{SC}_{Al_1}(x)$ or $E^{SC}_{Al_2}(x)$ is the total energy function with the SC structure. Thus, a series of partial cohesive energy curves corresponding to the interaction between identical atoms and distinct atoms have been obtained in the same way.

In this work, the total energies of different structures are obtained by the *ab initio* calculations using ESOCS program, which are provided by Materials Simulation Incorporation. The augmented spherical-wave method [17,18] and the local density functional theory are adopted. A series of total energies are calculated with various lattice constants at equal intervals of 0.1 Å. In each case, more than 80 k-points in an irreducible Brillouin zone are taken into account in a self-consistent calculation. The energy convergence error is 2×10^{-6} eV/atom.

2.2. Lattice inversion technique

In general, the cohesive energy, $E(x)$, for each atom in a crystal structure can be expressed as a sum of pair potential $\Phi(x)$, such that:

$$E(x) = \frac{1}{2}\sum_{Ri \neq 0} \Phi(R_i) = \frac{1}{2}\sum_{n=1}^{\infty} r_0(n)\Phi[b_0(n)x] \quad (3)$$

where x is the nearest neighbor interatomic distance, R_i is the lattice vector of the ith atom, $r_0(n)$ is the nth-neighbor coordination number, and $b_0(n)x$ is the nth neighbor distance. By a self-multiplicative process of the element in $b_0(n)$, the $b(n)$ forms a closed multiplicative semi-group, in which, for any arbitrary two integer m and n, there always exists an integer k, so that $b(k)=b(m)b(n)$. Then the general equation for the interatomic pair potential obtained from inversion could be expressed as

$$\Phi(x) = 2\sum_{n=1}^{\infty} I(n)E[b(n)x] \quad (4)$$

where $I(n)$, inversion coefficient, can be uniquely determined from the crystal structure as

$$\sum_{b(n)|b(k)} I(n) r\left[b^{-1}\left[\frac{b(k)}{b(n)}\right]\right] = \delta_{k1} \quad (5)$$

Note that the $I(n)$ is only structure dependent and is not related to concrete element category. Then the interatomic pair potentials can be obtained from the known cohesive energy function, $E(x)$. Fig. 1 gives several important relevant interatomic potentials of U–Fe–Al system as a function of the interatomic distance, r. These inverted pair potentials are approximately expressed as Morse function:

$$\Phi(x) = D_0\{\exp[-\alpha(r/R_0-1)] - 2\exp[-(\alpha/2)(r/R_0-1)]\} \quad (6)$$

where r is the distance between two atoms, and D_0, α and R_0 are potential parameters, which are given in Table 1.

As the inverted potentials are obtained by a strict lattice inversion of crystal cohesive energy curves, it can be deduced that the pair potentials could properly reproduced the cohesive energy, the bulk modulus and some other simple properties. This method has been applied successfully to study the site preference and lattice dynamics of rare-earth compounds with $CaCu_5$-type compounds and their derivatives [19–24]. Moreover, the technique was also used to investigate the properties of transition metal

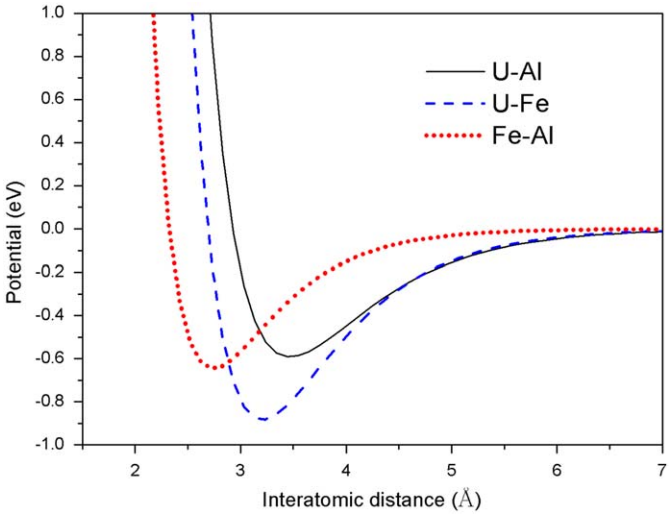

Fig. 1. Potential curves of $\Phi_{U-Fe}(r)$, $\Phi_{U-Al}(r)$ and $\Phi_{Fe-Al}(r)$.

Table 1
Morse parameters of the inverted pair potentials.

	R_0 (Å)	D_0 (eV)	α
Y–Y	4.079	0.514	8.716
Ru–Ru	2.941	0.941	10.103
Al–Al	3.006	0.423	8.919
U–U	3.942	0.662	7.345
U–Ru	3.306	1.058	8.558
Th–Ru	3.387	0.981	8.848
U–Al	3.468	0.592	8.871
U–Fe	3.202	0.884	8.684
Th–Fe	3.308	0.757	8.586
Th–Al	3.644	0.534	8.851

carbides and nitrides [12,25–28]. Therefore, this rigorous and concise inversion technology is adopted in this work, and we could simulate multi-elemental systems with a large cell, e.g. $(U_3Fe_{4+x}Al_{12-x})_{2\times2\times4}$.

3. Results and discussion

3.1. Crystal structure of $R_3T_4Al_{12}$

Ternary aluminides with the formula $R_3T_4Al_{12}$ crystallize in the hexagonal $Gd_3Ru_4Al_{12}$-type structure, which were first determined by Gladyshevskii et al. [4]. There are 6 rare earth atoms and 32 metal atoms located at seven different symmetry sites of space group $P6_3/mmc$. The crystal structure of $R_3T_4Al_{12}$ could be considered as two kinds of layer stacking up along the hexagonal c axis. Fig. 2 shows the two kinds of layer (I) and (II). As previously described [4,10], T atoms in the layer (I) form a series of triangular meshes, and the centers of meshes are located by Al atoms either approximately in the plane (Al-4f) or above or below the plane (Al-12k). R atoms in the layer (II) are located at the apexes of triangles on one side; Al (6h) atoms are arranged in the equilateral triangles on the other side.

The structural stabilities and lattice constants of $R_3T_4Al_{12}$ (R=Y, Ce, Gd, U, Th; T=Fe, Ru) compounds are studied by a series of tests. If the inverted potentials are effective and reasonable, they might make the deformed structures recover to the equilibrium phase with the lowest energy. The deformed structures were reconstructed by random atom shifts (RAS) and global deformations (GD). In the RAS tests, the atoms in the crystal are randomly shifted up to a certain distance from its equilibrium positions. In the GD tests, some operations (such as stretching, compressing, shearing and a combination of these) are performed on the initial model. All these distorted structures are taken into the force fields, which are set up by a series of interatomic potentials, and then the energy minimization procedures are performed. As shown in Table 2, over quite a large range of deformations, the structures of $Y_3Fe_4Al_{12}$ can return to the same crystal parameters as before, i.e., the final structure is stable over quite a large range of phase space. Based on the final stable structure, the lattice constant and cohesive energy could be acquired, and the calculated results of $R_3T_4Al_{12}$ (R=Y, Ce, Gd, U, Th; T=Fe, Ru) are listed in Table 3 together with experimental data from the literature [3–5,9,10]. It can be seen that our results agree with the experimental data and the deviations are less than 4%. These results testify that the potentials here are effective and reasonable for these ternary compounds.

3.2. Site preference of $R_3T_{4+x}Al_{12-x}$

The transition metal atoms (T) could substitute for Al atoms in a rather large extent in the R–T–Al systems, and what we

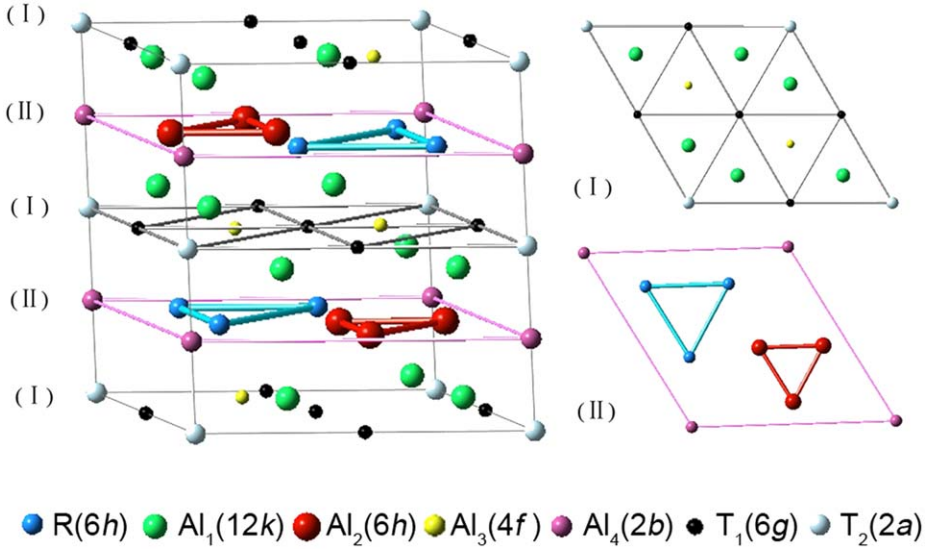

Fig. 2. Crystal structure of $R_3T_4Al_{12}$.

Table 2
The structural stability of $Y_3Fe_4Al_{12}$.

Parameters for deformation structure			Can these parameters return to the original ones[a]
a, b, c (Å)	α, β, γ (deg)	Space group	
10,10,12	90,90,120	$P6_3/mmc$	Yes
6,6,5	90,90,120	$P6_3/mmc$	Yes
8.8,8.8,9.4	80,70,100	$P1$	Yes
8.8,8.8,9.4	100,90,90	$P1$	Yes
4,5,7	80,90,110	$P1$	Yes
9,10,11	90,95,140	$P1$	Yes
Atoms random-shift 0.2 Å		$P1$	Yes
Atoms random-shift 0.4 Å		$P1$	Yes
Atoms random-shift 0.6 Å		$P1$	Yes

[a] Original parameters: a=b=8.817 Å, c=9.364 Å, α=β=90°, γ=120°, and the space group is $P6_3/mmc$.

Table 3
Comparison of calculated lattice parameters and energy with experimental data.

Compounds	a (Å)			c (Å)			E (eV/atom)
	Cal.	Exp.	Err. (%)	Cal.	Exp.	Err. (%)	
$Y_3Fe_4Al_{12}$	8.817			9.364			−4.569
$Ce_3Fe_4Al_{12}$	8.942			9.537			−4.412
$Gd_3Fe_4Al_{12}$	8.969			9.434			−3.946
$U_3Fe_4Al_{12}$	8.852	8.752[a]	1.14	9.433	9.265[a]	1.81	−5.066
	8.852	8.745[b]	1.22	9.433	9.259[b]	1.88	
$Th_3Fe_4Al_{12}$	9.096			9.713			−4.646
$Y_3Ru_4Al_{12}$	9.032	8.777[c]	2.91	9.708	9.523[c]	1.94	−4.864
$Ce_3Ru_4Al_{12}$	9.136	8.865[d]	3.05	9.831	9.570[d]	2.73	−4.751
$Gd_3Ru_4Al_{12}$	9.137			9.869			−4.362
$Gd_3Ru_{4.13}Al_{11.87}$	9.134	8.814[e]	3.63	9.865	9.569[e]	3.09	−4.396
$U_3Ru_4Al_{12}$	9.036			9.711			−5.373
$Th_3Ru_4Al_{12}$	9.215			9.835			−5.214

[a] Ref. [10].
[b] Ref. [9].
[c] Ref. [5].
[d] Ref. [3].
[e] Ref. [4].

concerned is which site may be the most stable position for T atoms in the process of substitution. Generally, the energy is an important criterion for the reason that the system with lower energy would be more stable than that with higher energy. Another criterion is the tolerance, which characterizes the deviation of the atomic position distribution. In a crystal with certain space group, each atom should occupy the symmetry site specifically. Ternary addition will cause a deviation of the atoms from the ideal sites and the tolerance increase significantly. When the tolerance increases to a certain extent, the crystal symmetry is fully destroyed, and the structure cannot form a stable phase with the previous space group. In our experience, the phase is unstable and the structure would not exist in experiment when the tolerance exceeds 0.6 Å. As a result, the tolerance criterion and the energy criterion are adopted in this work.

The calculation is performed with a supper-cell of 16 formula units, and T atoms substitute for Al atoms at each site with different concentrations. Then the energy minimization method is applied to relax the system under the interaction of potentials. In order to reduce statistical fluctuation, 20 samples are taken for each case with the equivalent Al sites randomly occupied by T atoms.

The calculated average energies and tolerances of $U_3Fe_{4+x}Al_{12-x}$ and $Th_3Fe_{4+x}Al_{12-x}$ are shown in Fig. 3 when Fe atoms occupy the 2*b*, 4*f*, 6*h* and 12*k* sites, respectively. The figure clearly shows that all the tolerances are less than 0.6 Å, which indicate that all the compositions after substitution belong to the $Gd_3Ru_4Al_{12}$-type structure. The average energies decrease when Fe atoms substitute for Al atoms at each of the four sites, which mean that the addition of Fe atoms increases the stability of U–Fe–Al systems. Further, the energy decreases most significantly while Fe atoms preferentially occupy the 6*h* sites, the energy decreases less significantly if Fe atoms occupy 4*f* sites, and even less corresponding to 2*b* and 12*k* sites. Therefore, Fe atoms preferentially occupy the 6*h* site based on the lowest average energy and the acceptable tolerance.

The calculated tolerances of $U_3Ru_{4+x}Al_{12-x}$ and $Th_3Ru_{4+x}Al_{12-x}$ are plotted in Fig. 4. It can be seen form the figure that the tolerances are much larger than 0.6 Å when Ru atoms occupy the 2*b*, 4*f* and 12*k* sites, which means that the crystal symmetry is destroyed and the phase is unstable in each case. Only when the Ru atoms substitute for Al atoms at 6*h* sites, the tolerances would decrease. As a result, the Ru atoms would occupy 6*h* sites during the substitution based on the tolerance consideration. The final average energies of $U_3Ru_{4+x}Al_{12-x}$ and $Th_3Ru_{4+x}Al_{12-x}$ are decrease with the increase of Ru content, which indicate that Ru atoms can also play a role in stabilizing the structure.

The calculated result shows that T (T=Fe, Ru) atoms preferentially occupy 6*h* sites, which is consistent with experiments derived from X-ray powder diffraction data [4,10]. As can be seen from Fig. 2, the Al (6*h*) sites with a slight substitution by T atoms are arranged in the equilateral triangles on the plane (II) together with the rare earth triangles.

3.3. Elastic properties of $R_3T_4Al_{12}$

Generally, the mechanical properties of these ternary compounds can hardly be measured experimentally due to their brittleness and low symmetry. Also, a huge computer resource is required to calculate them by an *ab initio* method because of their complex structures. In this work, the elastic constants and bulk moduli of $R_3T_4Al_{12}$ (R=Y, Ce, Gd, U, Th; T=Fe, Ru) have been calculated by the inverted interatomic potentials. The results are listed in Table 4. It can be seen from the table that $U_3Fe_4Al_{12}$ has the largest bulk modulus of all the Fe-based aluminides, and $U_3Ru_4Al_{12}$ has the largest bulk modulus of all the Ru-based aluminides. In general, the $R_3T_4Al_{12}$ compounds possess similar mechanical properties.

3.4. Vibrational properties of $R_3T_4Al_{12}$

Phonon density of states (DOS) reflects the lattice dynamic properties, and the derived specific heat and vibrational entropy are important thermodynamic parameters. Based on the effective potentials and lattice dynamic theory, the phonon DOS of $R_3Fe_4Al_{12}$ (R=Y, Ce, Gd, U, Th) are calculated by considering the contribution to the DOS of the distinct atoms. Note that the phonon DOS and thermodynamic properties of these compounds with $Gd_3Ru_4Al_{12}$-type structure are first evaluated at an atomistic level. Fig. 5 shows the calculated total phonon DOS of $U_3Fe_4Al_{12}$ and $Th_3Fe_4Al_{12}$ as well as the partial DOS of different elements. It can be seen that Al atoms offer the dominant vibrational modes in the high frequency region. Fe atoms largely contribute to modes with lower frequencies. U atoms and Th atoms, however, only contributes to modes below 4.00 THz.

In the present work, the localized modes have been analyzed qualitatively from the interatomic potentials by considering the

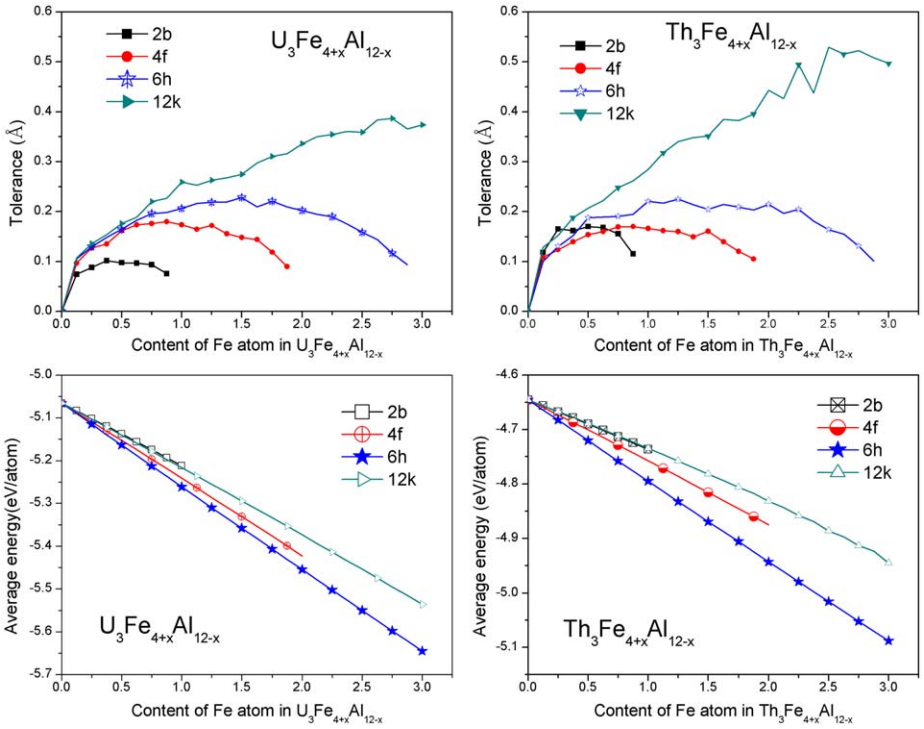

Fig. 3. Tolerance and average energy variations with x when Fe atoms occupy different sites in $U_3Fe_{4+x}Al_{12-x}$ and $Th_3Fe_{4+x}Al_{12-x}$.

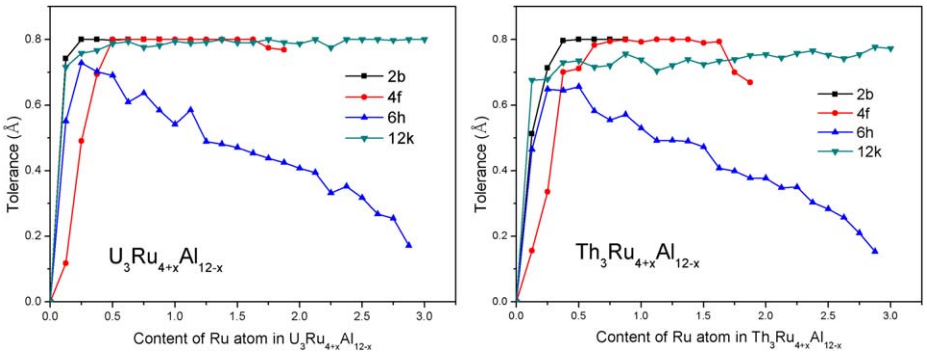

Fig. 4. Tolerance variations with x when Ru atoms occupy different sites in $U_3Ru_{4+x}Al_{12-x}$ and $Th_3Ru_{4+x}Al_{12-x}$.

Table 4
Elastic constants and bulk moduli of $R_3T_4Al_{12}$ (R=Y, Ce, Gd, U, Th; T=Fe, Ru).

Compounds	Elastic constants C_{ij} (GPa)						Bulk modulus (GPa)
	C_{11}	C_{12}	C_{13}	C_{33}	C_{44}	C_{66}	
$Y_3Fe_4Al_{12}$	311	117	71	351	67	97	166
$Ce_3Fe_4Al_{12}$	296	108	80	366	73	94	166
$Gd_3Fe_4Al_{12}$	338	135	83	405	74	101	187
$U_3Fe_4Al_{12}$	349	131	92	412	83	109	193
$Th_3Fe_4Al_{12}$	279	116	75	316	62	82	156
$Y_3Ru_4Al_{12}$	285	157	69	365	56	64	170
$Ce_3Ru_4Al_{12}$	284	139	76	382	66	73	170
$Gd_3Ru_4Al_{12}$	302	152	77	355	65	75	174
$U_3Ru_4Al_{12}$	332	168	86	433	74	82	198
$Th_3Ru_4Al_{12}$	294	166	78	399	68	64	181

nearest neighbors. Take $U_3Fe_4Al_{12}$ as an example. The U–U bond distance is 3.52 Å, which is longer than the other bond distances, indicating a weak bonding interaction between them. The neighbors of a U atom are 11 Al atoms, and the distances range from 3.08 to 3.22 Å. The distance between U and its nearest Fe is 3.32 Å. It can be seen from Fig. 1 that U reacts strongly with Fe and Al at these distances. The mass of U is much larger than that of Al and is thus assumed motionless relative to the Al atom. Some Al atoms are restricted to the 'potential well' $\phi_{u-Al}(r)$. This might be the reason for the appearance of Al-localized modes that correspond to the higher transected frequency. U atoms only contribute to lower frequency vibrations because of their large atomic mass. The interaction between U and Fe is intense at their closest point (3.32 Å). However, Fe atoms could not excite more modes with higher frequency compared to Al atoms due to the heavy mass of Fe. It should be noticed that the nearest distance between Fe and Al is 2.36 Å, indicating very strong interaction between these two atoms. This means that the Al atoms contribute to higher frequency modes than Fe atoms because of the light Al atoms.

The Phonon DOS of $R_3Ru_4Al_{12}$ (R=Y, Ce, Gd, U, Th) are similar with that of $U_3Fe_4Al_{12}$. The total vibrational modes could be marked as three parts: Al atoms offer the dominant vibrational modes with highest frequency, Ru atoms excite the localized modes with lower frequency, and the rare earth atoms only contribute the localized modes below 4.5 THz.

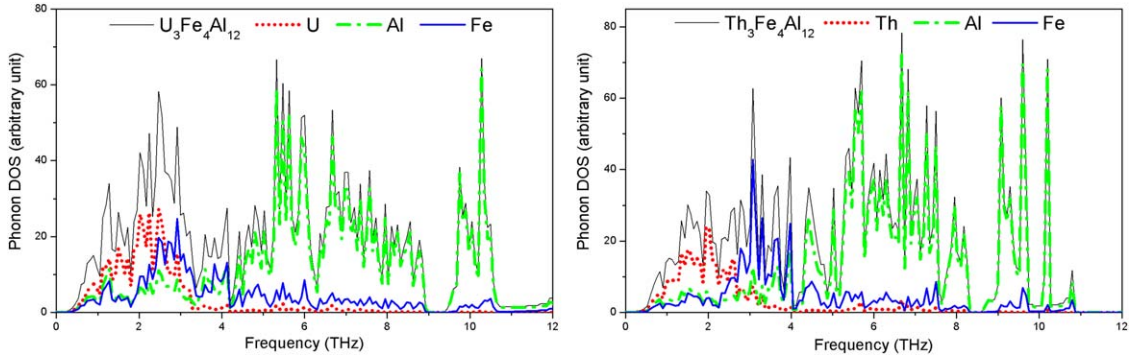

Fig. 5. Phonon DOS of $U_3Fe_4Al_{12}$ and $Th_3Fe_4Al_{12}$.

The Debye temperature of a material is a suitable parameter to describe phenomena of solid-state physics that associated with lattice vibrations. In this section, the lattice specific heat, $C_V(T)$, is calculated by following formula:

$$C_V(T) = 3Nk_B \int_0^{\infty} \frac{(\hbar\omega/k_BT)^2 e^{\hbar\omega/k_BT}}{(e^{\hbar\omega/k_BT}-1)^2} g(\omega)\, d\omega \tag{7}$$

where $g(\omega)$ is total DOS. In the conventional Debye model, the Debye temperature Θ_D can be defined as $\hbar\omega_m/k_B$, the specific heat can be written as

$$C_V(T) = 3Nk_B(T/\Theta_D)^3 \int_0^{\Theta_D/T} \frac{x^4 e^x}{(e^x-1)^2} dx \tag{8}$$

where $x = \hbar\omega/k_BT$. The Debye temperature could be calculated through the formulas above based on the total vibrational DOS. The Debye temperatures of $U_3Fe_4Al_{12}$ and $Th_3Fe_4Al_{12}$ are 295 and 267 K, respectively. Unfortunately, in the existing literature, there are no experimental data on the Debye temperature of these compounds.

4. Conclusion

The structural properties of $R_3T_{4+x}Al_{12-x}$ (R=Y, Ce, Gd, U, Th; T=Fe, Ru) with $Gd_3Ru_4Al_{12}$-type structure have been investigated by using a series of interatomic pair potentials acquired from lattice inversion method. The energies and space groups of the ternary systems are calculated based on the long-range interaction between atoms, and used as the criterion for site preference. Calculated results demonstrate that T atoms would substitute for Al atoms preferentially at 6*h* sites. The calculated lattice constants coincide with the experimental data. Furthermore, the lattice vibrational properties of $R_3Fe_4Al_{12}$ have been evaluated, and the contributions of different elements to the total phonon density of states are analyzed qualitatively with the relevant potentials.

The method utilized in the present investigation offers a rather easy and direct way to investigate the structural properties of complex compounds. The main advantage is that these potentials are directly extracted from *ab initio* calculations without any experimental data and a priori potential function forms, which reduce some uncertainties in the derivation of potentials. However, the pair potentials are not universal for any atomistic simulation due to the inherent disadvantage, especially in solving the problems such as defects, surface vacancies etc. The three-body potentials and many-body potentials should be considered. These issues call for further study.

Acknowledgments

The authors express their deep gratitude to Professor Y. Liu, P. Qian and X. J. Yuan for interesting discussions and encouragement. This work is supported by the National Basic Research Program of China (Grant No. 2006CB605101) and the National Natural Science Foundation of China (Grant No. 50971024).

References

[1] K.H.J. Buschow, J. Alloys Comp. 193 (1993) 223–230.
[2] D. Kaszorowski, P. Rogl, K. Hiebl, Phys. Rev. B 54 (1996) 9891–9902.
[3] N.G. Bukhan'ko, A.I. Tursina, S.V. Malyshev, A.V. Gribanov, Yu.D. Seropegin, O.I. Bodak, J. Alloys Comp. 367 (2004) 149–151.
[4] R.E. Gladyshevskii, O.R. Strusievicz, K. Cenzual, E. Parthé, Acta Crystallogr. B 49 (1993) 474–478.
[5] J. Niermann, W. Jeitschko, Z. Anorg. Allg. Chem. 628 (2002) 2549–2556.
[6] O. Tougait, H. Noël, R. Troc, J. Solid State Chem. 177 (2004) 2053–2057.
[7] H. Noël, O. Tougait, R. Troc, V. Zaremba, Solid State Sci. 7 (2005) 780–783.
[8] P. Qian, H.J. Tian, N.X. Chen, J. Shen, J. Solid State Chem. 181 (2008) 983–986.
[9] A.P. Goncalves, H. Noël, Intermetallics 13 (2005) 580–585.
[10] A.P. Goncalves, J.C. Waerenborgh, P. Gaczyński, H. Noël, O. Tougait, Intermetallics 17 (2009) 25–31.
[11] Y.H. Luo, Y.Z. Wang, Phys. Rev. A 64 (2001) 015201.
[12] J.Y. Xie, N.X. Chen, J. Shen, L.D. Teng, S. Seetharaman, Acta Mater. 53 (2005) 2727–2732.
[13] A.E. Carlsson, C.D. Gelatt, H. Ehrenreich, Phil. Mag. A 41 (1980) 241.
[14] N.X. Chen, Phys. Rev. Lett. 64 (1990) 1193.
[15] N.X. Chen, Z.D. Chen, Y.C. Wei, Phys. Rev. E 55 (1997) R5.
[16] N.X. Chen, Curr. Opin. Solid State Mater. Sci. 10 (2006) 15.
[17] A.R. Williams, J. Kübler, C.D. Gelatt, Phys. Rev. B 19 (1979) 6094–6118.
[18] V.L. Moruzzi, C.B. Sommers, Calculated Electronic Properties of Ordered Alloys, World Scientific, Hackensack, NJ, 1995.
[19] P. Qian, N.X. Chen, J. Shen, J. Phys. D Appl. Phys. 39 (2006) 1197–1203.
[20] J. Shen, P. Qian, N.X. Chen, Model. Simul. Mater. Sci. Eng. 13 (2005) 239–247.
[21] P. Qian, N.X. Chen, J. Shen, Model. Simul. Mater. Sci. Eng. 13 (2005) 851–860.
[22] Y. Chen, J. Shen, Acta Phys. Sin. 58 (2009) S141.
[23] Y. Chen, J. Shen, Acta Phys. Sin. 58 (2009) S146.
[24] P. Qian, W. Su, J. Shen, N.X. Chen, Comput. Mater. Sci. 43 (2008) 319–324.
[25] J.Y. Xie, N.X. Chen, L.D. Teng, S. Seetharaman, Acta Mater. 53 (2005) 5305–5312.
[26] J.Y. Xie, J. Shen, N.X. Chen, S. Seetharaman, Acta Mater. 54 (2006) 4563–4568.
[27] Y. Chen, J. Shen, N.X. Chen, Solid State Commun. 149 (2009) 121–125.
[28] Y. Chen, J. Shen, N.X. Chen, Chin. Phys. Lett. 26 (2009) 048101.